Breast ultrasound tomography with two parallel transducer arrays: Preliminary clinical results

Lianjie Huang[a], Junseob Shin[a], Ting Chen[a], Youzuo Lin[a], Miranda Intrator[a], Kenneth Hanson[a], Katherine Epstein[b], Daniel Sandoval[b], and Michael Williamson[b]

[a]Los Alamos National Laboratory, Los Alamos, NM 87545, USA;
[b]University of New Mexico, Department of Radiology, Albuquerque, NM 87131, USA

ABSTRACT

Ultrasound tomography has great potential to provide quantitative estimations of physical properties of breast tumors for accurate characterization of breast cancer. We design and manufacture a new synthetic-aperture breast ultrasound tomography system with two parallel transducer arrays. The distance of these two transducer arrays is adjustable for scanning breasts with different sizes. The ultrasound transducer arrays are translated vertically to scan the entire breast slice by slice and acquires ultrasound transmission and reflection data for whole-breast ultrasound imaging and tomographic reconstructions. We use the system to acquire patient data at the University of New Mexico Hospital for clinical studies. We present some preliminary imaging results of *in vivo* patient ultrasound data. Our preliminary clinical imaging results show promising of our breast ultrasound tomography system with two parallel transducer arrays for breast cancer imaging and characterization.

Keywords: Breast cancer, synthetic-aperture ultrasound, ultrasound imaging, ultrasound tomography.

1. INTRODUCTION

Ultrasound tomography (UST) was developed as a potential quantitative imaging tool in 1970s with the pioneering work of Greenleaf et al.[1,2] and Carson et al.[3] A number of UST prototype systems were developed to study the imaging capability of UST for breast cancer detection and diagnosis.[4–10] The working principle of UST is similar to X-ray CT (computed tomography) while the ionizing radiation in X-ray CT is replaced by ultrasound in UST. Synthetic-aperture ultrasound acquires ultrasound reflection/transmission data scattered from different directions.[11–18] It is a promising imaging modality for improving medical ultrasound imaging and tomography.[9,15–42]

Ultrasound bent-ray tomography reconstructs the sound-speed and ultrasound attenuation distributions within the breast.[8,43–51] One of the primary advantages of ultrasound bent-ray tomography is its computational efficiency that could lead to almost real-time imaging using GPU computers.[40] However, ultrasound bent-ray tomography can only produce low-resolution images, and could fail to image highly heterogeneous, dense breasts. This requires ultrasound waveform tomography that can properly handle complex wave phenomena in heterogeneous, dense breasts. With the increasing computing power, ultrasound waveform tomography is becoming feasible. We recently developed a suite of new ultrasound waveform tomography algorithms for improving the tomography robustness and computational efficiency.[38,42,52–55]

We design and manufacture a breast ultrasound tomography system to study the capability of ultrasound bent-ray and waveform tomography using both ultrasound transmission and reflection data. The system uses two parallel linear transducer arrays with a total of 768 transducer elements and 384 parallel receive channels to acquire synthetic-aperture ultrasound data. The distance between the two arrays is adjustable for scanning different sizes of breasts. We calibrate the motion control system to ensure that the two ultrasound transducer arrays are aligned to each other at each vertical position when scanning patients. We use the breast ultrasound tomography system to scan patients at the University of New Mexico Hospital and acquire ultrasound transmission and reflection data for ultrasound imaging and tomography.

We describe our custom-built breast ultrasound tomography prototype, give the calibration result of the motion control system, outline the strategy for patient recruitment, and present some preliminary imaging and tomography results of patient data to demonstrate the feasibility of the system for patient studies.

Send correspondence to Lianjie Huang: ljh@lanl.gov

Medical Imaging 2015: Ultrasonic Imaging and Tomography, edited by Johan G. Bosch,
Neb Duric, Proc. of SPIE Vol. 9419, 941916 · © 2015 SPIE
CCC code: 1605-7422/15/$18 · doi: 10.1117/12.2082404

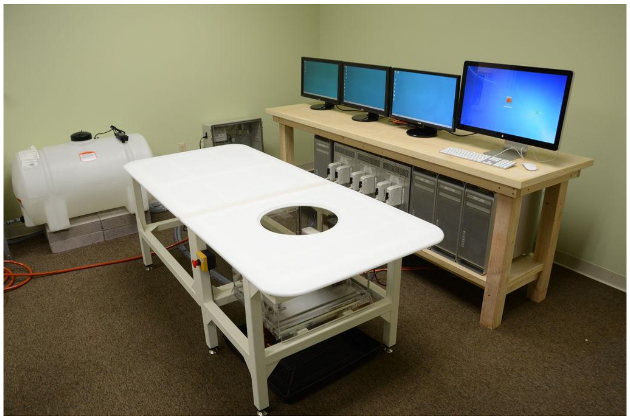

(a) Breast ultrasound tomography prototype.

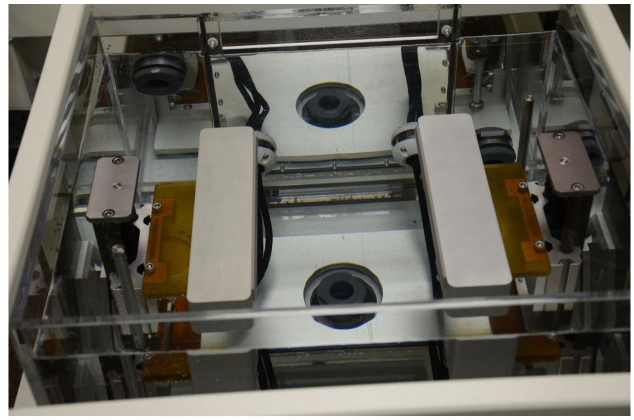

(b) Two parallel ultrasound transducer arrays.

Figure 1: LANL's custom-built breast ultrasound tomography system with 768 ultrasound transducer elements and 384 parallel receive channels for acquiring synthetic-aperture ultrasound data.

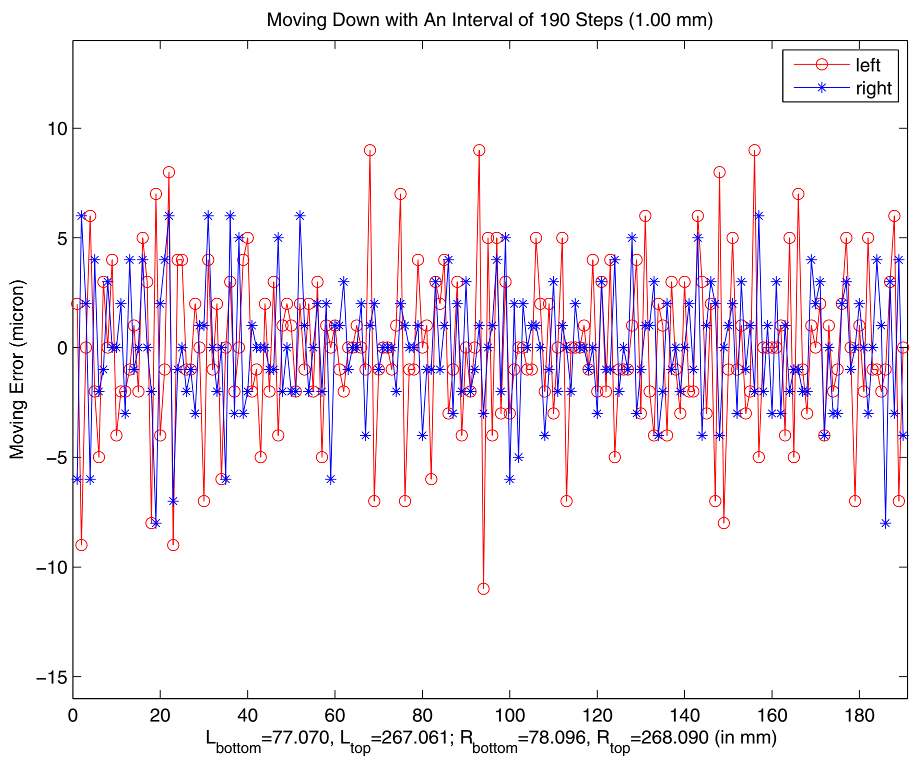

Figure 2: The differences between the vertical positions of the two ultrasound transducer arrays after motion position adjustment when the transducer arrays move from a top position of the linear motion stage downward for 190 mm. Most position differences are within 5 μm.

2. BREAST ULTRASOUND TOMOGRAPHY PROTOTYPE

We design and manufacture an ultrasound tomography prototype to acquire synthetic-aperture ultrasound data. The prototype as shown in Fig. 1(a) consists of two parallel transducer arrays, a motion control system with two linear motion stages, an imaging water tank, a storage water tank with warm water, a water filtering system, a water degassing system, a data acquisition system, a master PC computer to control the operation of the entire system, and a table bed for patients to lie down in the prone position for ultrasound tomography scanning. We have custom-built parts from various companies and assemble them together as a working system.

The two parallel transducer arrays displayed in Fig. 1(b) comprise a total of 768 transducer elements firing ultrasound at the center frequency of 1.875 MHz. Each linear motion stages moves one ultrasound transducer arrays a small vertical step before/after scanning one slice. The two ultrasound transducer arrays are aligned to each other at each vertical scanning position. The distance between the two parallel transducer arrays is adjustable to optimally scan breasts with different sizes.

The data acquisition system has 384 parallel receive channels to record ultrasound data. To acquire synthetic-aperture ultrasound data, each transducer element is fired sequentially, and all transducer elements receive ultrasound transmission/reflection/scattering signals.

Patient lies on the table bed in the prone position and one breast is immersed into the warm water tank. The breast not only is centered between the ultrasound transducer arrays, but also is aligned at the middles of the ultrasound transducer arrays. The entire breast is scanned slice by slice using the two ultrasound transducer arrays when they moves vertically with a small interval. It takes approximately 2.5 seconds to scan one slice, including times to move and align the ultrasound transducer arrays, scan the breast, and store ultrasound data to hard drives for imaging and image reconstructions.

3. CALIBRATION OF THE MOTION CONTROL SYSTEM

It is essential to minimize the offset between the moving distances between the two linear motion stages in order to align the two ultrasound transducer arrays. During scanning of each slice, we first move each transducer array to the desired vertical position. However, the real transducer array positions may not be at the expected locations. The maximum position error is up to 60 μm. We adjust the transducer positions around the desired vertical position for each array until their position difference is within 10 μm. We move the ultrasound transducer arrays from a top position downward for 190 mm with an vertical step interval of 1 mm. Figure 2 shows that most position errors are within 5 μm. The moving speed of the linear motion stages measured without the position adjustment is approximately one millimeter per second. With our motion error control procedure, the averaged moving speed is approximately 1.5 seconds per millimeter.

4. ULTRASOUND IMAGING AND TOMOGRAPHY WITH *IN VIVO* PATIENT DATA

We install our custom-built clinical breast ultrasound tomography system at the University of New Mexico Outpatient Surgery-Imaging Services building in Albuquerque, New Mexico, for clinical studies. After installation, the system is tested and inspected for patient safety by University of New Mexico Hospitals' Clinical Engineers, New Mexico State Department of Health, other personnel, and is approved for scanning patients under a clinical research protocol approved by the University of New Mexico Institutional Review Board (IRB).

Our plan is to recruit a total of 200 patients for this clinical ultrasound tomography study to evaluate the capability of breast ultrasound tomography for characterizing breast tumors.

4.1 Patient recruitment

We recruits patients from those with breast symptoms or recently abnormal screening mammograms, or abnormality findings from other conventional imaging modalities such as clinical ultrasound and MRI, and they requires an additional evaluation.

The mammographer, who identifies a patient in need of follow-up clinical imaging for abnormalities for standard clinical reasons, notify the study personnel/coordinator that this patient may be eligible for the study. When the patient arrives for her clinical imaging appointment, the study personnel asks the patient whether she would be interested in the possibility of participating in the ultrasound tomography research project. The study personnel reads a recruitment script to potential participants, answers questions, and arranges to have consent administered either after the potential participant finishes their scheduled clinical imaging, which takes approximately 45 minutes to 1.5 hours, or on a separate scheduled visit. The subject has at the minimum 45-90 minutes to decide whether they would like to participate, along with the option to take the consent form home.

At the time of the patient's follow-up clinical appointment or scheduled study appointment, she is consented in a private area. The study personnel provides interested patients with a consent form. The consent form is reviewed with the patient and the patient is given ample opportunity to ask questions. To ensure understanding, the study personnel asks the patient to explain the study in their own words.

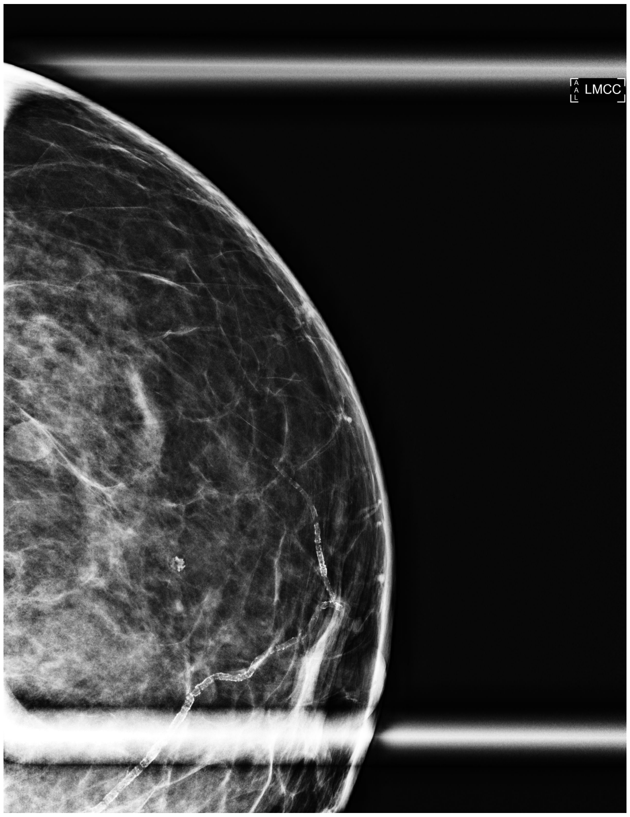

(a) Mammogram with a cyst.

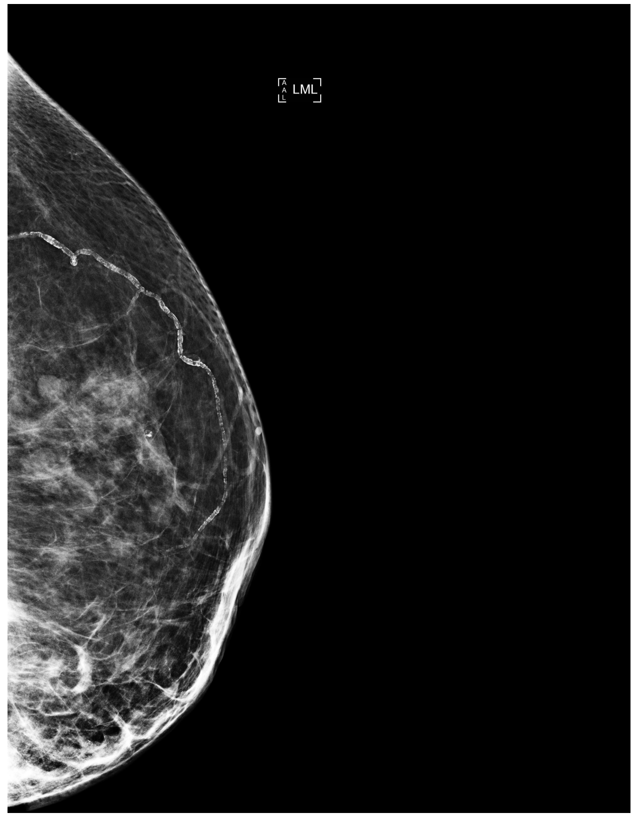

(b) Mammogram with a mass.

Figure 3: Two mammograms of Patient A shows a cyst in (a) and a solid mass in (b).

The study personnel emphasizes to the patient that their decision to participate does not affect their right to medical care. No UST scan is taken place prior to completion of the consent process

During the consent process, the patient is also provided with patient education materials, informing the patient what to expect from the new UST scanning device from the perspective of our patient advocates. The patient is also provided contact information of our patient advocates in case she wants to communicate with our patient advocates.

After the UST scan is complete, the patient is given a thank-you card and a questionnaire. The questionnaire allows us to gather information regarding the scanning experience from the patient's point of view, and allows us to improve the UST scan experience for other potential participants and patients in the future.

We present some preliminary ultrasound imaging and tomography results for two patients scanned using our clinical UST prototype.

4.2 Ultrasound Imaging for Patient A

Patient A is recruited for this UST study because her left breast has several cysts and a partially circumscribed, partially obscured mass. Fig. 3 shows two mammograms of the patient: one shows a cyst, and the other shows a solid mass. A targeted clinical ultrasound image of Patient A as displayed in Fig. 4(a) shows a simple cyst. This patient has a partially circumscribed, partially obscured mass in posterior depth. A targeted ultrasound image of this patient in Fig. 4 demonstrates a corresponding isoechoic and hypoechoic oval avascular mass with an indistinct margin. This is a suspicious mass, warranting tissue sampling.

The study personnel scans Patient A using LANL's UST machine and acquires synthetic-aperture ultrasound data. Figure 5 shows two coronal sections of beamforming images of the data. In Fig. 5, the point "0" along the azimuthal axis is the center position of the two parallel ultrasound transducer arrays, and both end elements of the two transducer arrays on the head side are at approximately -105 mm. Because this is the first patient scanned using our UST machine and the

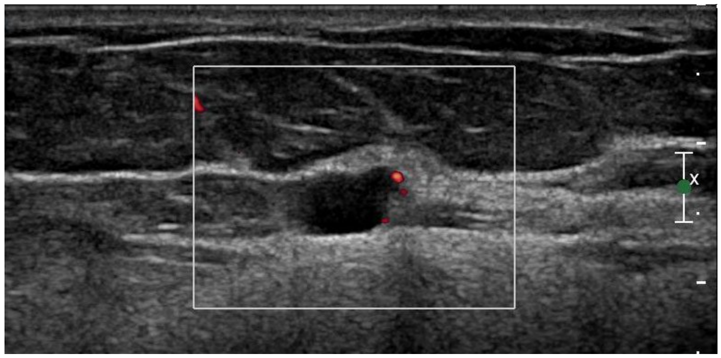

(a) Clinical ultrasound image shows a cyst within the boxed region.

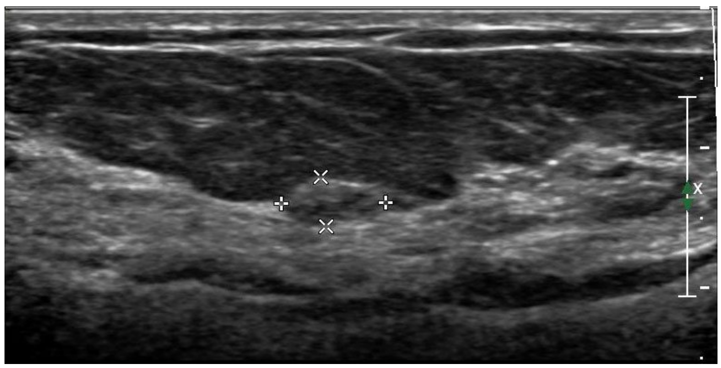

(b) Clinical ultrasound image shows a mass within the marked region.

Figure 4: Clinical ultrasound images of Patient A show a cyst within the boxed region in (a) and a solid mass within the marked region in (b).

study personnel lacks of experience to position the breast near the center of the imaging domain, the breast of Patient A is placed near one half of the ultrasound transducer arrays, leading to incomplete images in the top parts of the coronal images shown in Fig. 5. Nevertheless, the breast is mostly imaged, and the imaging result shows that the dark region in Figure 5(a) near the location at (Azimuthal, Axial) = (-50, 156) could be one of the cysts. The image abnormality shown near the center of the image in Figure 5(b) could be the suspicious mass.

4.3 Ultrasound Imaging and Tomography for Patient B

Patient B is recruited because her left breast has a fibroadenoma shown on her targeted ultrasound image within a boxed region in Fig. 6. The beamforming image obtained with synthetic-aperture ultrasound data acquired using our UST machine is displayed in Fig. 7. The fibroadenoma can be clearly identified on this coronal image.

We conduct ultrasound bent-ray tomography using the synthetic-aperture UST data for Patient B. Fig. 8 is a preliminary result of ultrasound bent-ray tomography.

5. CONCLUSIONS

We have designed and manufactured a breast ultrasound tomography system for clinical patient studies. The system consists of two parallel transducer arrays with a total of 768 transducer elements and 384 parallel receive channels. The center frequency of the ultrasound transducer arrays is 1.875 MHz. The distance between the two transducer arrays is adjustable for scanning different sizes of breasts. Two linear motion stages moves the two ultrasound transducer arrays vertically step by step to acquire patient ultrasound tomography data slice by slice. The position differences between the two transducer arrays are mostly within 5 μm, enabling us to accurately align the two transducer arrays to each other during each slice of scanning. The system takes approximately 2.5 seconds to scan each slice, including times to move the ultrasound transducer arrays, fire all 768 elements sequentially and record all ultrasound reflection and transmission

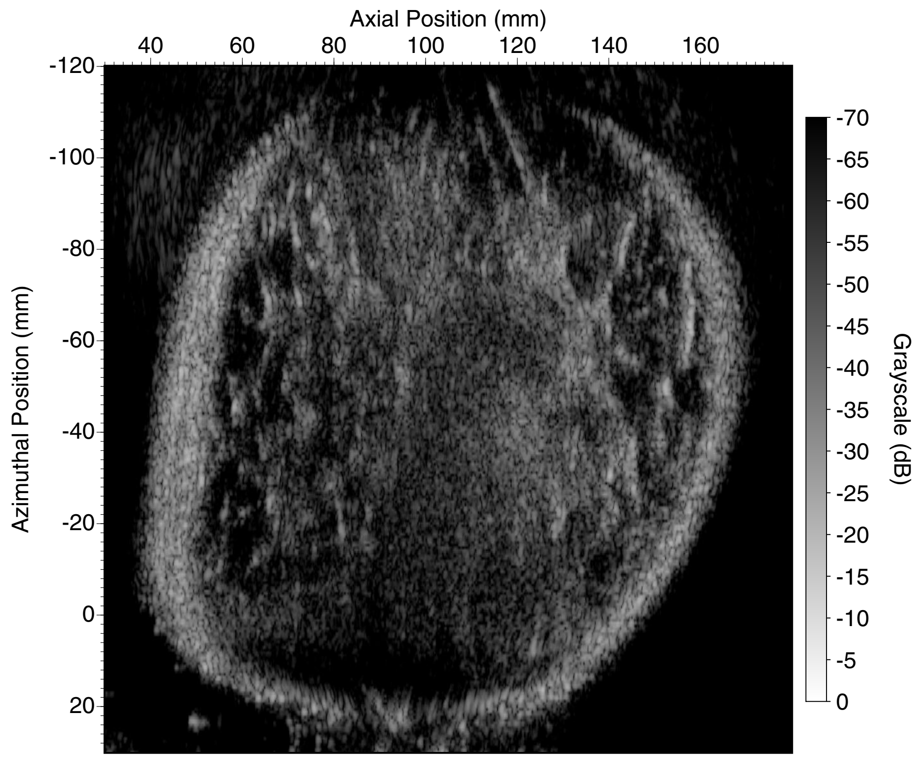

(a) A coronal section of ultrasound beamforming image.

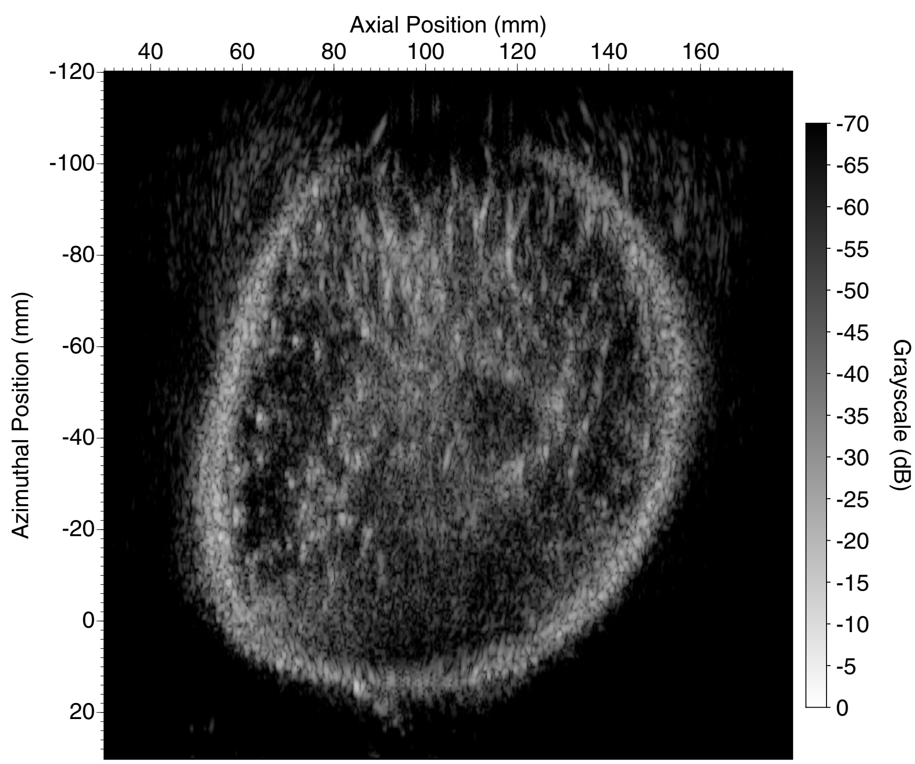

(b) A coronal section of ultrasound beamforming image.

Figure 5: Two coronal sections of ultrasound beamforming images of Patient A produced with synthetic-aperture ultrasound data acquired using LANL's ultrasound tomography prototype with two parallel transducer arrays.

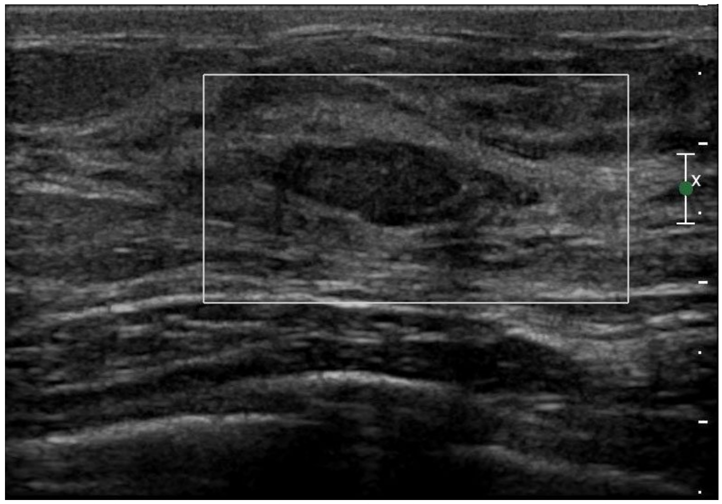

Figure 6: A targeted clinical ultrasound image of Patient B shows a solid mass within the breast.

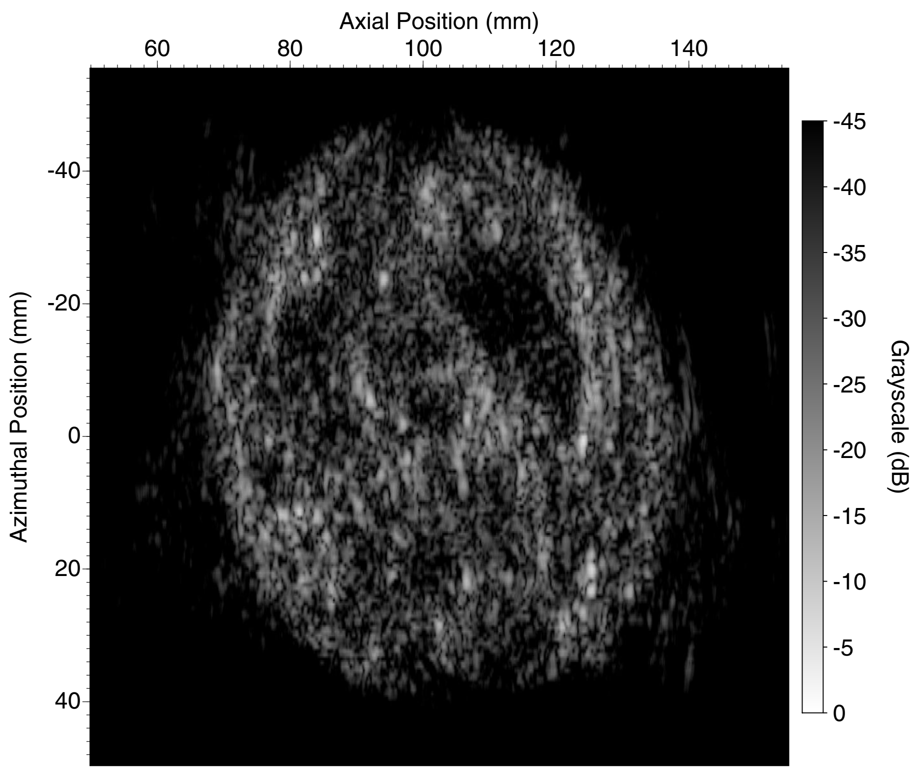

Figure 7: A coronal section of ultrasound beamforming images of Patient B produced with synthetic-aperture ultrasound data acquired using LANL's ultrasound tomography prototype with two parallel transducer arrays.

data, and store ultrasound data. We have used our custom-built breast ultrasound tomography system to scan patients at the University of New Mexico Outpatient Surgery-Imaging Services building, and produced ultrasound beamforming and bent-ray tomography images. Our preliminary clinical imaging results show promising of our breast ultrasound tomography system with two parallel transducer arrays for breast cancer imaging and characterization.

6. ACKNOWLEDGMENTS

This work was supported by the Breast Cancer Research Program of U.S. DOD Congressionally Directed Medical Research Programs. The computation was performed using super-computers of the Institutional Computing Program of Los Alamos

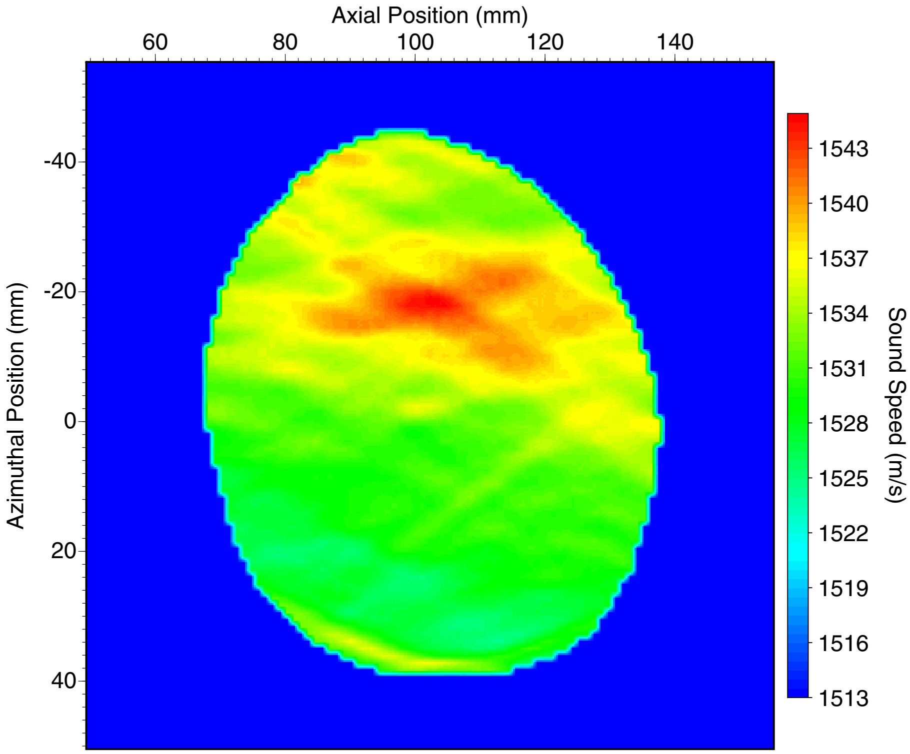

Figure 8: A coronal section of ultrasound bent-ray tomography images of Patient B produced with synthetic-aperture ultrasound data acquired using LANL's ultrasound tomography prototype with two parallel transducer arrays.

National Laboratory. We thank patient advocates Erin Bouquin, Peggy Devine, Elizabeth Harris, and Nancy Hawkins for their strong support and help during the course of this project.

REFERENCES

[1] Greenleaf, J., Johnson, S., Lee, S., Hermant, G., and Woo, E., "Algebraic reconstruction of spatial distributions of acoustic absorption within tissue from their two-dimensional acoustic projections," in [*Acoustical Holography*], Green, P., ed., 591–603, Springer US (1974).

[2] Greenleaf, J., Johnson, S., Samayoa, W., and Duck, F., "Algebraic reconstruction of spatial distributions of acoustic velocities in tissue from their time-of-flight profiles," in [*Acoustical Holography*], Booth, N., ed., 71–90, Springer US (1975).

[3] Carson, P. L., Meyer, C. R., Scherzinger, A. L., and Oughton, T. V., "Breast imaging in coronal planes with simultaneous pulse echo and transmission ultrasound," *Science* **214**, 1141–1143 (1981).

[4] Waag, R. C., Liu, D.-L., Mast, T. D., Nachman, A. I., Jaeger, P., and Kojima, T., "An ultrasonic ring transducer system for studies of scattering and imaging," *J. Acoust. Soc. Am.* **100**, 2795 (1996).

[5] Andre, M. P., Janee, H. S., Martin, P. J., Otto, G. P., Spivey, B. A., and Palmer, D. A., "High-speed data acquisition in a diffraction tomography system employing large-scale toroidal arrays," *International Journal of Imaging Systems and Technology* **8**, 137–147 (1997).

[6] Wiskin, J. W., Borup, D. T., and Johnson, S. A., "Inverse scattering from arbitrary two-dimensional objects in stratified environments via a green's operator," *Journal of the Acoustical Society of America* **102**, 853–864 (1997).

[7] Marmarelis, V. Z., Kim, T. S., and Shehada, R. E. N., "High resolution ultrasonic transmission tomography," in [*Ultrasonic Imaging and Signal Processing*], Walker, W. F. and Insana, M. F., eds., *Proc. SPIE* **5035**, 33–40, SPIE, Bellingham, Washington (2002).

[8] Duric, N., Littrup, P., Poulo, L., Babkin, A., Pevzner, R., Holsapple, E., and Rama, O., "Detection of breast cancer with ultrasound tomography: First results with the computerized ultrasound risk evaluation (cure) prototype," *Med. Phys.* **34**, 773–785 (2007).

[9] Duric, N., Littrup, P., Roy, O., Li, C., Schmidt, S., Cheng, X., and Janer, R., "Clinical breast imaging with ultrasound tomography: A description of the softvue system," *The Journal of the Acoustical Society of America* **135**(4), 2155–2155 (2014).

[10] Ruiter, N. V., Zapf, M., Hopp, T., Dapp, R., Kretzek, E., Birk, M., Kohout, B., and Gemmeke, H., "3d ultrasound computer tomography of the breast: A new era?," *European Journal of Radiology* **81**, S133–134 (2012).

[11] O'Donnell, M. and Thomas, L. J., "Efficient synthetic aperture imaging from a circular aperture with possible application to catheter-based imaging," *IEEE Transactions on Ultrasonics, Ferroelectrics, and Frequency Control* **39**, 366–380 (1992).

[12] Lockwood, G., Talman, J., and Brunke, S., "Real-time 3-d ultrasound imaging using sparse synthetic aperture beamforming," *IEEE Trans. Ultrason. Ferroelectr. Freq. Control* **45**, 980–988 (1998).
[13] Nikolov, S., Gammelmark, K., and Jensen, J., "Recursive ultrasound imaging," *Proceedings of the IEEE Ultrasonic Symposium* **2**, 1621–1625 (1999).
[14] Nikolov, S. I., *Synthetic aperture tissue and flow ultrasound imaging*, PhD thesis, Technical University of Denmark (2001).
[15] Jensen, J., Holm, O., Jensen, L., Bendsen, H., Nikolov, S., Tomov, B., Munk, P., Hansen, M., Salomonsen, K., Hansen, J., Gormsen, K., Pedersen, H., and Gammelmark, K., "Ultrasound research scanner for real-time synthetic aperture data acquisition," *IEEE Trans. Ultrason. Ferroelectr. Freq. Control* **52**, 881–891 (2005).
[16] Huang, L., Duric, N., and Littrup, P., "Breast imaging with time-reversed ultrasound," *Proc. SPIE* **6147**, 156–167 (2006).
[17] Jensen, J., Nikolov, S., Gammelmark, K., and Pedersen, M., "Synthetic aperture ultrasound imaging," *Ultrasonics* **44**, e5–e15 (2006).
[18] Daher, N. and Yen, J., "2-d array for 3-d ultrasound imaging using synthetic aperture techniques," *IEEE Trans. Ultrason. Ferroelectr. Freq. Control* **53**, 912–924 (2006).
[19] Huang, L., Duric, N., and Littrup, P., "Ultrasonic breast imaging using a wave-equation migration method," *Proc. SPIE* **5035**, 432–439 (2003).
[20] Simonetti, F., "Multiple scattering: The key to unravel the subwavelength world from the far-field pattern of a scattered wave," *Physical Review E* **73**, 036619–1–13 (2006).
[21] Huang, L. and Quan, Y., "Ultrasound pulse-echo imaging using the split-step Fourier propagator," *Proc. SPIE* **6513**, 651305–1–12 (2007).
[22] Pratt, R. G., Huang, L., Duric, N., and Littrup, P., "Sound-speed and attenuation of the breast tissue using waveform tomography of transmission ultrasound data," in [*Physics of Medical Imaging*], Hsieh, J. and Flynn, M. J., eds., *Proc. SPIE* **6510**, 65104S–1–12, SPIE, Bellingham, Washington (2007).
[23] Simonetti, F., Huang, L., Duric, N., and Rama, O., "Imaging beyond the born approximation: An experimental investigation with an ultrasonic ring array," *Physical Review E* **76**, 036601–1–10 (2007).
[24] Simonetti, F. and Huang, L., "From beamforming to diffraction tomography," *Journal of Applied Physics* **103**, 103110–1–7 (2008).
[25] Huang, L., Hanson, K. M., Quan, Y., Li, C., and Duric, N., "Globally optimized Fourier finite-difference method for ultrasound breast imaging," *Proc. SPIE* **6920**, 692007–1–11 (2008).
[26] Andresen, H., Nikolov, S., Pedersen, M., Buckton, D., and Jensen, J., "Three-dimensional synthetic aperture focusing using a rocking convex array transducer," *IEEE Trans. Ultrason. Ferroelectr. Freq. Control* **57**, 1051–1063 (2010).
[27] Huang, L., Simonetti, F., Huthwaite, P., Rosenberg, R., and Williamson, M., "Detecting breast microcalcifications using super-resolution and wave-equation ultrasound imaging: A numerical phantom study," in [*Ultrasonic Imaging, Tomography, and Therapy*], D'hooge, J. and McAleavey, S. A., eds., *Proc. SPIE* **7629**, 762919–1–10, SPIE (2010).
[28] Nikolov, S. I., Kortbek, J., and Jensen, J. A., "Practical applications of synthetic aperture imaging," in [*Proceedings – IEEE Ultrasonics Symposium*], 350–358 (2010).
[29] Huang, L., Labyed, Y., Simonetti, F., Williamson, M., Rosenberg, R., Heintz, P., and Sandoval, D., "High-resolution imaging with a real-time synthetic aperture ultrasound system: A phantom study," in [*Ultrasonic Imaging, Tomography, and Therapy*], D'hooge, J. and Doyley, M. M., eds., *Proc. SPIE* **7968**, 79681I–1–10, SPIE (2011).
[30] Labyed, Y. and Huang, L., "Detecting small targets using windowed time-reversal MUSIC imaging: A phantom study," *International Ultrasonics Symposium Proceedings* **10.1109/ULTSYM.2011.0392**, 1579–1582 (2011).
[31] Huang, L., Labyed, Y., Lin, Y., Zhang, Z., Pohl, J., Sandoval, D., and Williamson, M., "Detection of breast microcalcifications using synthetic-aperture ultrasound," in [*Ultrasonic Imaging, Tomography, and Therapy*], D'hooge, J. and Doyley, M. M., eds., *Proc. SPIE* **8320**, 83200H–1–8, SPIE (2012).
[32] Labyed, Y. and Huang, L., "Ultrasound imaging of extended targets using a windowed time-reversal MUSIC method," in [*Ultrasonic Imaging, Tomography, and Therapy*], D'hooge, J. and Doyley, M. M., eds., *Proc. SPIE* **8320**, 832019–1–10, SPIE (2012).
[33] Labyed, Y. and Huang, L., "Ultrasound time-reversal MUSIC imaging with diffraction and attenuation compensation," *IEEE Trans. Ultrason. Ferroelectr. Freq. Control* **59**, 2186–2200 (2012).
[34] Labyed, Y. and Huang, L., "Ultrasound time-reversal MUSIC imaging of extended targets," *Ultrasound in Med. & Biol.* **38**, 2018–2030 (2012).
[35] Huang, L., Labyed, Y., Hanson, K., Sandoval, D., Pohl, J., and Williamsonb, M., "Detecting breast microcalcifications using super-resolution ultrasound imaging: A clinical study," in [*Ultrasonic Imaging, Tomography, and Therapy*], Bosch, J. G. and Doyley, M. M., eds., *Proc. SPIE* **8675**, doi: 10.1117/12.2007653, 86751O–1–10, SPIE, Bellingham, Washington (2013).
[36] Labyed, Y. and Huang, L., "Super-resolution ultrasound phase-coherent MUSIC imaging with compensation for the phase response of transducer elements," *IEEE Trans. Ultrason. Ferroelectr. Freq. Control* **60**, 1048–1060 (2013).
[37] Labyed, Y. and Huang, L., "TR-MUSIC inversion of the density and compressibility contrasts of point scatterers," *IEEE Transactions on Ultrasonics, Ferroelectrics, and Frequency Control* **61**, 16–24 (2014).
[38] Lin, Y. and Huang, L., "Ultrasound waveform tomography with a spatially-variant regularization scheme," in [*Ultrasonic Imaging and Tomography*], Bosch, J. G. and Doyley, M. M., eds., *Proc. SPIE* **9040**, 90401M–1–7, SPIE, Bellingham, Washington (2014).
[39] Nguyen, N. Q. and Huang, L., "Ultrasound bent-ray tomography using both transmission and reflection data," in [*Ultrasonic Imaging and Tomography*], Bosch, J. G. and Doyley, M. M., eds., *Proc. SPIE* **9040**, 90400R–1–8, SPIE, Bellingham, Washington (2014).

[40] Labyed, Y. and Huang, L., "Toward real-time bent-ray breast ultrasound tomography using gpus," in [*Ultrasonic Imaging and Tomography*], Bosch, J. G. and Doyley, M. M., eds., *Proc. SPIE* **9040**, 90401N–1–8, SPIE, Bellingham, Washington (2014).
[41] Huang, L., Lin, Y., Zhang, Z., Labyed, Y., Tan, S., Nguyen, N., Hansona, K., Sandoval, D., and Williamson, M., "Breast ultrasound waveform tomography: Using both transmission and reflection data, and numerical virtual point sources," in [*Ultrasonic Imaging and Tomography*], Bosch, J. G. and Doyley, M. M., eds., *Proc. SPIE* **9040**, 90400T–1–12, SPIE, Bellingham, Washington (2014).
[42] Zhang, Z. and Huang, L., "Efficient implementation of ultrasound waveform tomography using data blending," in [*Ultrasonic Imaging and Tomography*], Bosch, J. G. and Doyley, M. M., eds., *Proc. SPIE* **9040**, 90401O–1–9, SPIE, Bellingham, Washington (2014).
[43] Littrup, P. J., Duric, N., Azevedo, S., Chambers, D. H., Candy, J. V., Johnson, S., Auner, G., Rather, J., and Holsapple, E. T., "Computerized Ultradound Risk Evaluation (CURE) system: Development of combined transmission and reflection ultrasound with new reconstruction algorithms for breast imaging," *Acoustical Imaging* **26**, 175–182 (2002).
[44] Littrup, P., Duric, N., Leach Jr., R. R., Azevedo, S. G., Candy, J. V., Moore, T., Chambers, D. H., Mast, J. E., and Holsapple, E. T., "Characterizing tissue with acoustic parameters derived from ultrasound data," in [*Ultrasonic Imaging and Signal Proceesing*], Insana, M. and Walker, W. F., eds., *Proc. SPIE* **4687**, 354–361, SPIE, Bellingham, Washington (2002).
[45] Duric, N., Littrup, P., Holsapple, E. T., Babkin, A., Duncan, R., Kalinin, A., Pevzner, R., and Tokarev, M., "Ultrasound tomography of breast tissue," in [*Ultrasonic Imaging and Signal Processing*], Walker, W. F. and Insana, M., eds., *Proc. SPIE* **5035**, SPIE, Bellingham, Washington (2003).
[46] Duric, N., Littrup, P. J., Rama, O., and Holsapple, E. T., "Computerized ultrasound risk evaluation (CURE): First clinical results," *Acoustical Imaging* **28** (2005).
[47] Quan, Y. and Huang, L., "Sound-speed tomography using first-arrival transmission ultrasound for a ring array," in [*Ultrasonic Imaging and Signal Processing*], Emelianov, S. Y. and McAleavey, S. A., eds., *Proc. SPIE* **6513**, doi: 10.1117/12.709647, 651306–1–9, SPIE, Bellingham, Washington (2007).
[48] Li, C., Duric, N., and Huang, L., "Clinical breast imaging using sound-speed reconstructions of ultrasound tomography data," in [*Ultrasonic Imaging and Signal Processing*], McAleavey, S. A. and D'hooge, J., eds., *Proc. SPIE* **6920**, 692009–1–9, SPIE (2008).
[49] Li, C., Duric, N., and Huang, L., "Comparison of ultrasound attenuation tomography methods for breast imaging," in [*Ultrasonic Imaging and Signal Processing*], McAleavey, S. A. and D'hooge, J., eds., *Proc. SPIE* **6920**, 692015–1–9, SPIE (2008).
[50] Li, C., Duric, N., Littrup, P., and Huang, L., "In vivo breast sound-speed imaging with ultrasound tomography," *Untrasound in Med. & Biol.* **35**, 1615–1628 (2009).
[51] Li, C., Huang, L., Duric, N., Zhang, H., and Rowe, C., "An improved automatic time-of-flight picker for medical ultrasound tomography," *Ultrasonics* **49**, 61–72 (2009).
[52] Lin, Y., Huang, L., and Zhang, Z., "Ultrasound waveform tomography with the total-variation regularization for detection of small breast tumors," in [*Ultrasonic Imaging, Tomography, and Therapy*], Bosch, J. G. and Doyley, M. M., eds., *Proc. SPIE* **8320**, doi: 10.1117/12.910765, 832002–1–9, SPIE, Bellingham, Washington (2012).
[53] Zhang, Z., Huang, L., and Lin, Y., "Efficient implementation of ultrasound waveform tomography using source encoding," in [*Ultrasonic Imaging, Tomography, and Therapy*], Bosch, J. G. and Doyley, M. M., eds., *Proc. SPIE* **8320**, doi: 10.1117/12.910969, 832003–1–10, SPIE, Bellingham, Washington (2012).
[54] Lin, Y. and Huang, L., "Ultrasound waveform tomography with a modified total-variation regularization scheme," in [*Ultrasonic Imaging, Tomography, and Therapy*], Bosch, J. G. and Doyley, M. M., eds., *Proc. SPIE* **8675**, doi: 10.1117/12.2007650, 86751F–1–9, SPIE, Bellingham, Washington (2013).
[55] Zhang, Z. and Huang, L., "Ultrasound waveform tomography using wave-energy-based preconditioning," in [*Ultrasonic Imaging, Tomography, and Therapy*], Bosch, J. G. and Doyley, M. M., eds., *Proc. SPIE* **8675**, doi: 10.1117/12.2007659, 86751G–1–10, SPIE, Bellingham, Washington (2013).